IVYSPRING INTERNATIONAL PUBLISHER

Theranostics

2019; 9(14): 4241-4254. doi: 10.7150/thno.35285

Research Paper

A Combination of Oxo-M and 4-PPBP as a potential regenerative therapeutics for tendon injury

Solaiman Tarafder, Christopher Ricupero, Sumeet Minhas, Rebecca J. Yu, Ashleigh D. Alex, Chang H. Lee✉

Columbia University College of Dental Medicine, 630 W. 168th street, Vanderbilt Clinic 12-210, New York, NY 10032

✉ Corresponding author: Chang H. Lee, PhD., Associate Professor, Regenerative Engineering Laboratory, Associate Director, Center for Advanced Regenerative Technologies, Columbia University Irving Medical Center, 630 W. 168 St. VC12-230, New York, NY 10032. Phone: 212-305-1920; Email: chl2109@cumc.columbia.edu

Received: 2019.03.28; Accepted: 2019.04.21; Published: 2019.05.31

Abstract

Tendons injuries frequently result in scar-like tissue with poor biochemical structure and mechanical properties. We have recently reported that CD146$^+$ perivascular originated tendon stem/progenitor cells (TSCs), playing critical roles in tendon healing. Here, we identified highly efficient small molecules that selectively activate endogenous TSCs for tendon regeneration.

Methods: From a pool of ERK1/2 and FAK agonists, Oxo-M and 4-PPBP were identified, and their roles in tenogenic differentiation of TSCs and *in vivo* tendon healing were investigated. Controlled delivery of Oxo-M and 4-PPBP was applied via PLGA μS. Signaling studies were conducted to determine the mechanism for specificity of Oxo-M and 4-PPBP to CD146$^+$ TSCs.

Results: A combination of Oxo-M and 4-PPBP synergistically increased the expressions of tendon-related gene markers in TSCs. *In vivo*, delivery of Oxo-M and 4-PPBP significantly enhanced healing of fully transected rat patellar tendons (PT), with functional restoration and reorganization of collagen fibrous structure. Our signaling study suggested that Oxo-M and 4-PPBP specifically targets CD146$^+$ TSCs via non-neuronal muscarinic acetylcholine receptors (AChR) and σ1 receptor (σ1) signaling.

Principal conclusions: Our findings demonstrate a significant potential of Oxo-M and 4-PPBP as a regenerative therapeutics for tendon injuries.

Key words: Tendon, Regenerative Medicine, Endogenous stem/progenitor cells, Small molecules

Introduction

Stem cell-based therapy has received tremendous attention in the hope of regenerating defective tissues or organs. For decades, stem cell-based regenerative therapies have predominantly focused on stem cell transplantation into the defect sites to replace damaged cells or to provide signals regulating healing process [1-4]. Prior to *in vivo* transplantation, stem cells need to be isolated from relevant sources, culture-expanded to achieve an enough cell number, and frequently directed to differentiate into a tissue-specific lineage [1-4]. Alternatively, it has been attempted to engineer tissue substitutes *in vitro* with stem cells, biomaterial scaffolds, and biochemical or physical stimuli [5-7]. Despite being a valid approach with promising research progress, stem cell transplantation with or without scaffolds and bioactive cues has encountered crucial barriers in therapeutic translation that include immune rejection, pathogen transmission, potential tumorigenesis, issues associated with packaging, storage, and shipping, and difficulties in clinical adoption and regulatory approval [2, 8-10]. Risk factors associated with the current stem cell based approaches for regenerative engineering include poorly understood in vivo fate of transplanted stem cells, low yield of engraftment, and potential loss of

regenerative capacity during *in vitro* culture [2, 8-10]. Given the limitations associated with stem cell transplantation, a need for new or advanced therapeutic approaches are emphasized. Recently, *in situ* tissue engineering by regulating recruitment and/or differentiation of endogenous stem cells has been proposed with a growing body of experimental support [1, 11-18].

In this study, we explored the potential of *in situ* tissue engineering approach for tendon regeneration by small molecules. Tendons are dense connective tissues with the primary function of transferring mechanical forces from muscle to bone. Tendon injuries, caused by laceration, contusion, or tensile overload are highly prevalent, accounting for about half of the 33 million musculoskeletal injuries in the U.S. [19-23]. More than 30% of Americans over 60 years of age experience rotator cuff injuries, with over 50,000 patients undergoing surgical repair each year [24-26]. Achilles tendinopathy affects 11% of regular runners [24], and 5 million new cases of tennis elbow (lateral epicondylitis) occur annually in the U.S. [24]. Undoubtedly, tendon injuries represent an acute healthcare burden in the U.S., with a total cost exceeding $30 billion per year [24, 27]. Unfortunately, tendon trauma in the adult does not spontaneously heal. At best, scar-like tissue is formed with somewhat high cellularity and disarrayed collagen fibers, failing to restore structural integrity, mechanical properties or functionality [23, 28]. Various cell types including tenocytes and dermal fibroblasts have been applied in tendon tissue engineering *in vitro* or in animal models [29-35]. Autologous cells from tendons are of limited availability and regenerative capability [36-38], and skin fibroblasts are readily available but do not fully attain the phenotypes of tenocytes [27]. Stem and progenitor cells including bone marrow-derived mesenchymal stem/progenitor cells (MSCs) and adipose-derived stem/progenitor cells (ADSCs) have also demonstrated their potential to improve tendon healing at various anatomical locations [39-41]. Despite the promising research progress, there is no stem cell-based regenerative therapy available for human patients for tendon healing, likely due to the commercialization and regulatory barriers in association with cell transplantation [36, 37, 42].

In order to overcome the limitations associated with the existing stem cell-based approaches, we devised a novel *in situ* tissue engineering approach for tendon regeneration by activating endogenous stem/progenitor cells [13]. Recently, we have identified perivascular originated tendon stem/progenitor cells (TSCs) playing essential roles in connective tissue growth factor (CTGF)-improved tendon healing [13]. CTGF delivery in full-transected rat patellar tendon (PT) led to reconstruction of collagen orientation and mechanical properties similar to the native PT by regulating proliferation and tenogenic differentiation of endogenous TSCs via FAK and ERK1/2 pathway [13]. Despite its promising function, CTGF suffers from several translational barriers including its unknown receptor, dose dependency and the wide range of functions in different cell types. Accordingly, we sought here to develop highly efficient and pharmacokinetic small molecules that selectively activate the tendon-resident stem/progenitor cells, consequently leading to tendon regeneration. Since no cell transplantation is required, the proposed approach hold promise to overcome the translational hurdles related with cell isolation, culture, and manipulation *in vitro*. In addition, small molecules specifically targeting selected signaling pathway may serve as focused therapeutics in comparison with delivery of stem cells, cytokines or growth factors. As compared to growth factors, small molecules have a number of distinct advantages: they are more convenient to use, they provide a higher degree of temporal and spatial control over protein function, they have no risk for cross-species contamination, and their effects can be fine-tuned by varying their concentrations and combinations [43]. Therefore, our findings described below may facilitate the development of therapeutic drug system targeting endogenous stem cells for tendon repair and regeneration [43].

Results

Synergistic effect of Oxo-M and 4-PPBP on induced tenogenic differentiation of TSCs

Given that our recent study identified FAK and ERK1/2 signaling to be involved in CTGF-induced tenogenic differentiation of $CD146^+$ TSCs [13], we performed pre-screening of small molecules as FAK or ERK1/2 agonists with a potential to guide tenogenic differentiation of TSCs. From a list of FAK and/or ERK1/2 agonists and related chemical compounds in literature and compound library [44], we found Oxotremorine M (Oxo-M) and PPBP maleate (4-PPBP) as potential inducers for tenogenic differentiation of TSCs (**Fig. 1A**). Upon 1 wk treatment, 4-PPBP (10 μM) increased the mRNA expressions of collagen type I (COL-I) and type III (COL-III), whereas Oxo-M (1 mM) increased tenascin-C (Tn-C), vimentin (VIM), and Scx expressions in rat TSCs (**Fig. 1B**). Despite the elevated expressions of certain genes, either Oxo-M or 4-PPBP alone showed only a modest increase in tendon-related gene expressions with no significant change in tenomodulin (TnmD) (**Fig. 1B**). When

combined together, however, Oxo-M and 4-PPBP induced 6 – 36 fold increases in the expressions of all the tested gene markers, including COL-I, COL-III, Tn-C, VIM, TnmD, and Scx (**Fig. 1B**). The elevated gene expressions by Oxo-M and 4-PPBP were on par with the level of gene expressions induced by 100 ng/mL CTGF [13] (**Fig. 1B**). To confirm the safety of Oxo-M and 4-PPBP as a potential therapy, we performed cytotoxicity test with live/dead assays. Upon treatment at 1X, 5X, and 10X effective concentrations (1 mM and 10 μm for Oxo-M and 4-PPBP, respectively), rat tendon cells showed over 97.5 - 99.5% cell viability up to 3 days (**Supplementary Fig. S1**).

Mechanism of Oxo-M and 4-PPBP induced tenogenic differentiation

Although Oxo-M and 4-PPBP are known as ERK1/2 and FAK agonists in multiple cell types, respectively, we performed a signaling study to confirm the involvement of FAK and ERK1/2 signaling in tenogenic differentiation of TSCs induced by Oxo-M and 4-PPBP. Activation of FAK and ERK1/2 signaling by Oxo-M and 4-PPBP in TSCs was confirmed by western blot and siRNA knockdown (KD). By 12 hours' treatment in TSCs, Oxo-M resulted in phosphorylation of ERK1/2, whereas 4-PPBP resulted in phosphorylation of FAK and ERK1/2 (**Fig. 2A**). With combined Oxo-M and 4-PPBP, both p-FAK and p-ERK1/2 bands were detected (**Fig. 2A**). In contrast, CD146$^-$ tendon cells (excluding TSCs) showed no p-FAK band when treated by Oxo-M, 4-PPBP, and Oxo-M + 4-PPBP (**Fig. 2A**), suggesting that Oxo-M and 4-PPBP selectively target TSCs. Consistently, the level of tendon-related gene expressions induced by Oxo-M and 4-PPBP in CD146$^-$ tendon cells was marginal (**Supplementary Fig. S2**) in comparison with CD146$^+$ TSCs (c.f. **Fig. 1B**). In addition, siRNA knockdown (KD) of FAK and ERK1/2 was performed following our established protocol [13]. Briefly, FAK and ERK1/2 KD was performed using Silencer® siRNA (100 nM) and Neon® transfection system (ThermoFisher) with pre-optimized electroporation conditions (1,400V; 20 mS; 2 pulses) that resulted in significant reduction of FAK and ERK1/2 mRNA expressions in comparison with scrambled siRNA and negative control without siRNA (**Fig. 2B & C**). The FAK and ERK1/2 KD significantly attenuated the Oxo-M and 4-PPBP-induced tendon related gene expressions by 1 wk (**Fig. 2D**).

Enhanced tendon healing by Oxo-M and 4-PPBP

Given the promising *in vitro* outcome, we applied Oxo-M and 4-PPBP for our established tendon healing model *in vivo* [13]. Briefly, patellar tendons (PT) of 12 wk-old Sprague-Dawley (SD) rats were fully transected, followed by delivery of Oxo-M (1 mM) and 4-PPBP (10 μM) via fibrin gel (50 mg/mL fibrinogen and 50 U/mL thrombin), as per our previous work [13]. After 2 wks, tendons without treatment ended up with a bulged up scarred healing (**Fig. 3A**) whereas Oxo-M and 4-PPBP delivery

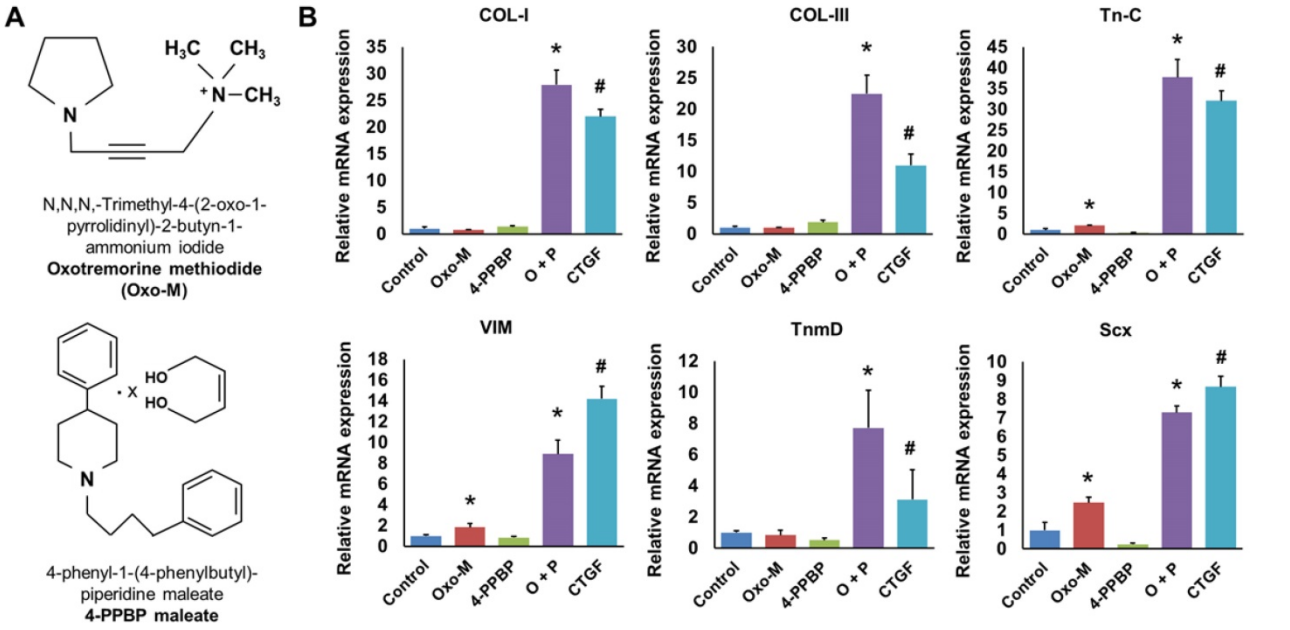

Fig. 1. Oxo-M and 4-PPBP (**A**) inducing tenogenic differentiation of TSCs via FAK and ERK1/2 signaling. Tendon-related gene expressions were induced in TSCs by 1 wk treatment of Oxo-M, 4-PPBP, and Oxo-M + 4-PPBP (O+P) (**B**). The treatment with 4-PPBP significantly increased COL-I and COL-III whereas Oxo-M increased Tn-C, VIM, and Scx. A combination of Oxo-M and 4-PPBP increased all the tested gene markers up to 8 – 38 folds on par with CTGF (n = 5 per group, *: p<0.001 compared to control, #: p<0.001 compared to all the other groups).

resulted in a native-like normal macroscopic structure of tendon (**Fig. 3B**). Histologically, delivery of Oxo-M and 4-PPBP resulted in a narrower healing gap than the control, Oxo-M alone, and 4-PPBP alone groups by 1 wk (**Fig. 3C & D**). By 2 wks, Oxo-M and 4-PPBP delivery significantly improved tendon healing with highly reoriented collagen fibers (**Fig. 3C & D**). In contrast, tendons in the control, Oxo-M alone and 4-PPPB alone delivered groups ended up with scar-like tissue healing featured by disrupted collagen structure and hypercellularity (**Fig. 3C & D**). In addition, the delivery of Oxo-M and 4-PPBP significantly increased the number of endogenous $CD146^+$ TSCs by 1 wk post-op that undergo differentiation into $proCOL\text{-}I^+$ tenocyte-like cells (**Fig. 3E**). Control, Oxo-M alone and 4-PPBP alone groups showed lack of $CD146^+$ TSCs by 1 wk post-op despite the hypercellularity in contrast to control, Oxo-M alone and 4-PPBP alone groups (**Fig. 3E**). Tendons healed with Oxo-M and 4-PPBP also showed a strong expression of Scx as compared to control, Oxo-M alone and 4-PPBP alone groups (**Fig. 3E**). Collagen contents quantified by imaging processing as per our established methods [45] were significantly higher in tendons with Oxo-M and 4-PPBP delivery (**Fig. 3F**). In addition, Oxo-M and 4-PPBP delivery significantly lower the cellularity in the healing tendons by 1 wk and 2 wks post-op, in comparison with the control, Oxo-M alone and 4-PPBP alone groups (**Fig. 3G**). Total cell numbers in 2 wks post-op were significantly lower than that of 1 wk post-op in all the groups (**Fig. 3G**).

Structural and functional restoration of tendons by Oxo-M and 4-PPBP

Analysis for collagen fibers orientation was performed by an automated imaging processing with circularly polarized Picrosirious red (PR) images (**Fig. 4A & B**) as per our established methods [13]. The densely aligned collagen fibers were shown in Oxo-M and 4-PPBP delivered tendons by 1 wk and 2 wks (**Fig. 4A**). Control, Oxo-M alone and 4-PPBP alone groups showed disrupted collagen structure with a lack of fiber alignment by 1 wk and 2 wks (**Fig. 4A**). Histograms for the fiber orientation angles indicated the densely aligned collagen fibers in Oxo-M and 4-PPBP delivered tendons similarly with native tendons, as compared to a lack of directional alignment in control, Oxo-M alone and 4-PPBP alone groups (**Fig. 4B**). Quantitatively, angular deviation (AD) of the fiber orientation was significantly lower with Oxo-M and 4-PPBP delivery than control, Oxo-M alone, and 4-PPBP alone (**Fig. 4B**) (n = 5 per group; $p<0.001$). Consistently, the tensile stiffness of healed PT with Oxo-M and 4-PPBP was significantly higher than that of the fibrin alone control group (**Fig. 4C**) (n = 5 each group; $p<0.001$).

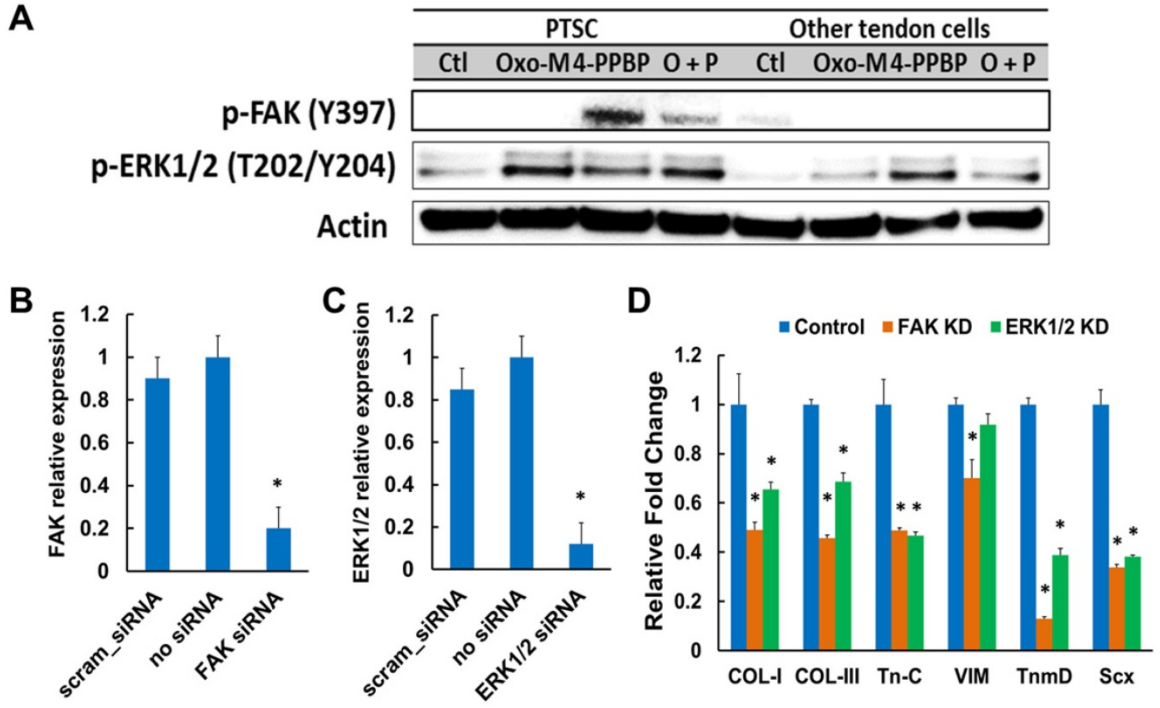

Fig. 2. Western blot show FAK and ERK phosphorylation induced by Oxo-M and 4-PPBP (**A**). siRNA transfection of FAK and ERK significantly reduced FAK and ERK1/2 mRNA expressions as compared to scrambled siRNA and no siRNA controls (**B & C**) (n = 5 per group; *: $p<0.001$ compared to all the other groups). FAK and ERK1/2 knockdown (KD) significantly attenuated the Oxo-M and 4-PPBP induced expressions of tendon-related gene (**D**) (n = 5 per group; *: $p<0.001$ compared to control – scrambled siRNA).

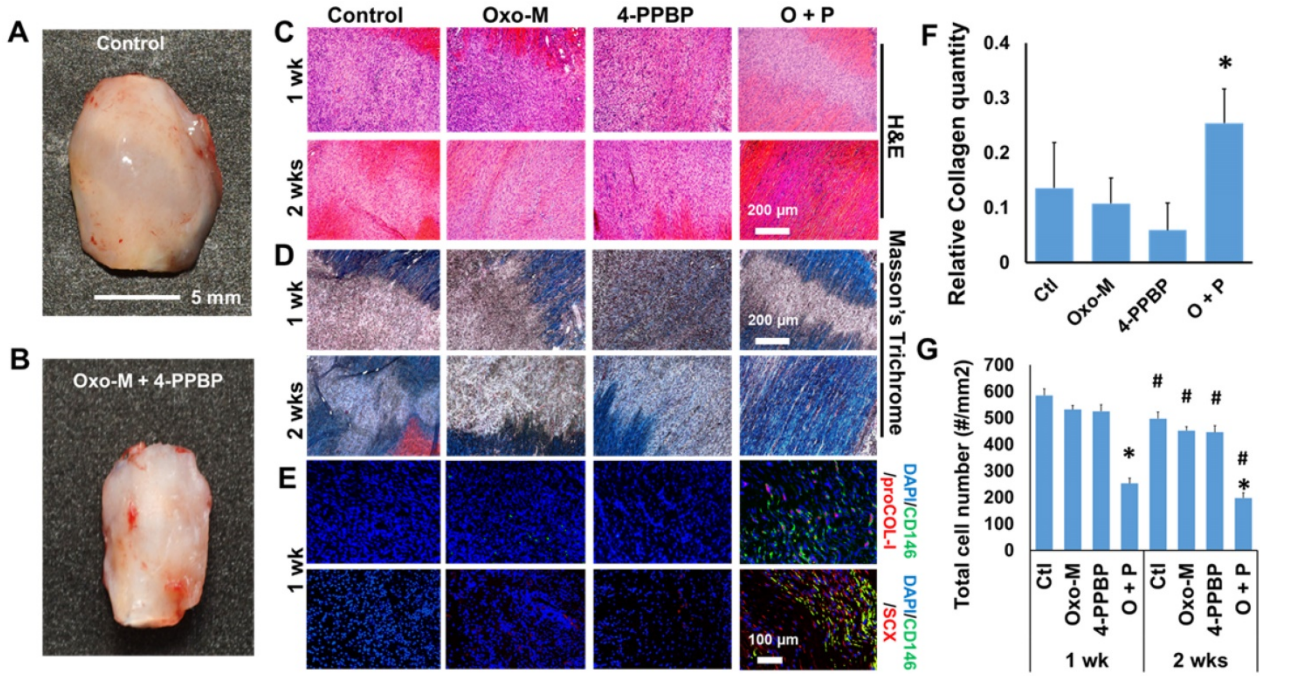

Fig. 3. Tendon healing by Oxo-M and 4-PPBP. In contrast to the enlarged scarred healing in control (**A**), Oxo-M and 4-PPBP delivery resulted in native-like tendon by 2 wks (**B**). H&E (**C**) and Masson's Trichrome staining (**D**) further showed that Oxo-M and 4-PPBP delivery improved tendon healing with reorganized collagen fibers in comparison with disrupted scar-like tissues with control, Oxo-M, or 4-PPBP alone. Immunofluorescence show the increased number of endogenous CD146$^+$ TSCs undergoing tenogenic differentiation expressing proCOL-I and Scx by 1 wk post-op in comparison with control, Oxo-M alone and 4-PPBP alone (**E**). Relative collagen quantity from imaging processing was significantly higher with Oxo-M and 4-PPBP delivery (**F**). Total cell numbers were significantly lower with Oxo-M and 4-PPBP delivery than control, Oxo-M alone or 4-PPBP alone by 1 wk (**G**) (n = 10 sections per tissue sample; *: p<0.01 compared to other groups in the same time point; #: p<0.01 compared to 1 wk data).

Controlled delivery of Oxo-M and 4-PPBP to further improve tendon healing

Although Oxo-M and 4-PPBP showed a superior efficiency on the induction of *in vitro* tenogenic differentiation of TSCs over CTGF (**Fig. 1B**), *in vivo* functional tendon restoration by Oxo-M and 4-PPBP delivered via fibrin gel was at ~83.4% of native tendons (**Fig. 3C**). Oxo-M and 4-PPBP have small molecular weights (Mw 322.19 and Mw 293.45, respectively) that is likely attributed to the quick release from fibrin gel (<24 hours) in comparison with CTGF (38 kDa; release in 1 wk) [46]. Accordingly, we established a controlled delivery of Oxo-M and 4-PPBP for sustained releases to further improve tendon healing. Following our well-established methods [14, 46, 47], Oxo-M and 4-PPBP were encapsulated in biodegradable poly(lactic-co-glycolic acids) (PLGA) microspheres (μS) by double-emulsion technique (**Fig. 5A**). To measure released dose of Oxo-M and 4-PPBP from PLGA μS, we determined the maxima absorption (λ_{max}) as 230 nm and 207 nm for Oxo-M and 4-PPBP, respectively, from a series of measurements with UV-VIS spectroscopy (**Fig. 5B**). Oxo-M and 4-PPBP concentrations via measurements at each $\lambda_{max,}$ showed sustained release up to 8 days (**Fig. 5C**). To confirm bioactivities of Oxo-M and 4-PPBP release, PLGA μS-encapsulated with Oxo-M and 4-PPBP were placed on transwell whereas TSCs plated on the bottom wells. By 2 wks, applying Oxo-M and 4-PPBP μS in transwell resulted in substantial collagen deposition by TSCs cultured on the bottom substrate as compared to empty μS, Oxo-M μS alone and 4-PPBP μS alone (**Fig. 5D**), suggesting that released Oxo-M and 4-PPBP stimulated collagen production. When applied in our full-transected rat PT healing model, Oxo-M μS and 4-PPBP μS (10 mg/ml each) delivered via fibrin gel resulted in a further improved collagen formation and reorientation by 1 and 2 wks, as compared to scar-like healing in control (fibrin alone) (**Fig. 6A**). Histologically, delivery of Oxo-M μS and 4-PPBP μS resulted in denser collagen fibers than the delivery of Oxo-M and 4-PPBP via fibrin gel (**Fig. 6A**). In addition, the quantitative imaging analysis with the PR-stained images showed an enhanced collagen organization with Oxo-M μS and 4-PPBP μS with a narrower angular distribution in comparison with Oxo-M and 4-PPBP delivered via fibrin gel (**Fig. 6B**). The AD was significantly lower in Oxo-M μS and 4-PPBP μS delivery than Oxo-M and 4-PPBP via fibrin and control (**Fig. 6C**) (n= 5 per group; p<0.01). Consistently, the tensile stiffness of tendons delivered with Oxo-M μS and 4-PPBP μS were significantly higher than Oxo-M and 4-PPBP delivered tendons via fibrin, on a par with native level (**Fig. 6D**) (n=5 per group; p<0.01).

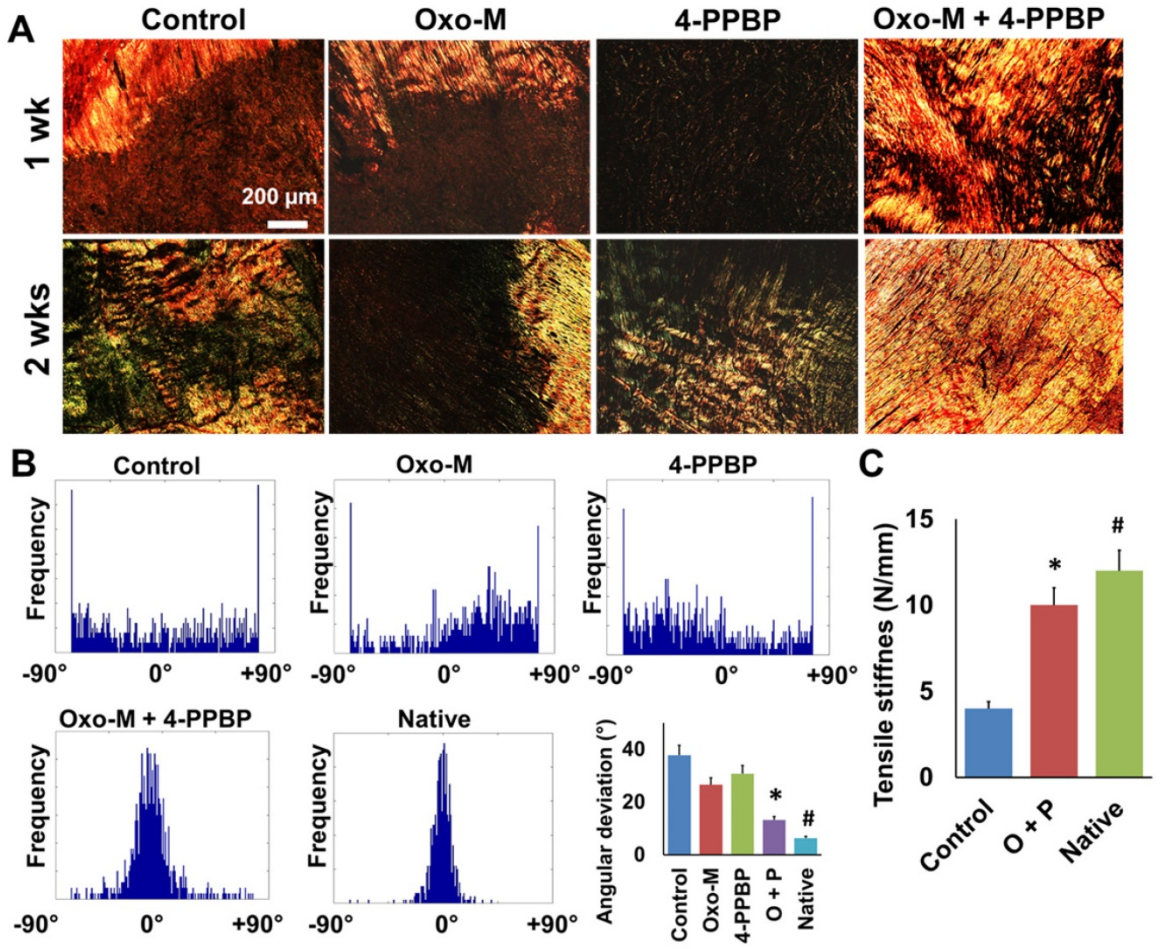

Fig. 4. Circular-polarized image of Picrosirius Red (PR) stained tendon sections (**A**) showed densely aligned collagen fibers with Oxo-M and 4-PPBP delivery. Automated digital image processing demonstrated narrower fiber orientation with Oxo-M and 4-PPBP similar to native (**B**). In contrast, control, Oxo-M alone and 4-PPBP alone showed spread histogram of angular orientation of collagen fibers (**B**). Quantitatively, angular deviation (AD) was significantly lower with Oxo-M and 4-PPBP delivery in comparison with control, Oxo-M alone, and 4-PPBP alone (**B**) (n = 6 per group; *: p<0.001 compared to control, Oxo-M, and 4-PPBP, #:p<0.05 compared to Oxo-M + 4-PPBP). Consistently, tensile stiffness was significantly higher with Oxo-M and 4-PPBP as compared to control (**C**) (n = 5 per group, *: p<0.001 compared to control, #: p<0.001 compared to Oxo-M + 4-PPBP).

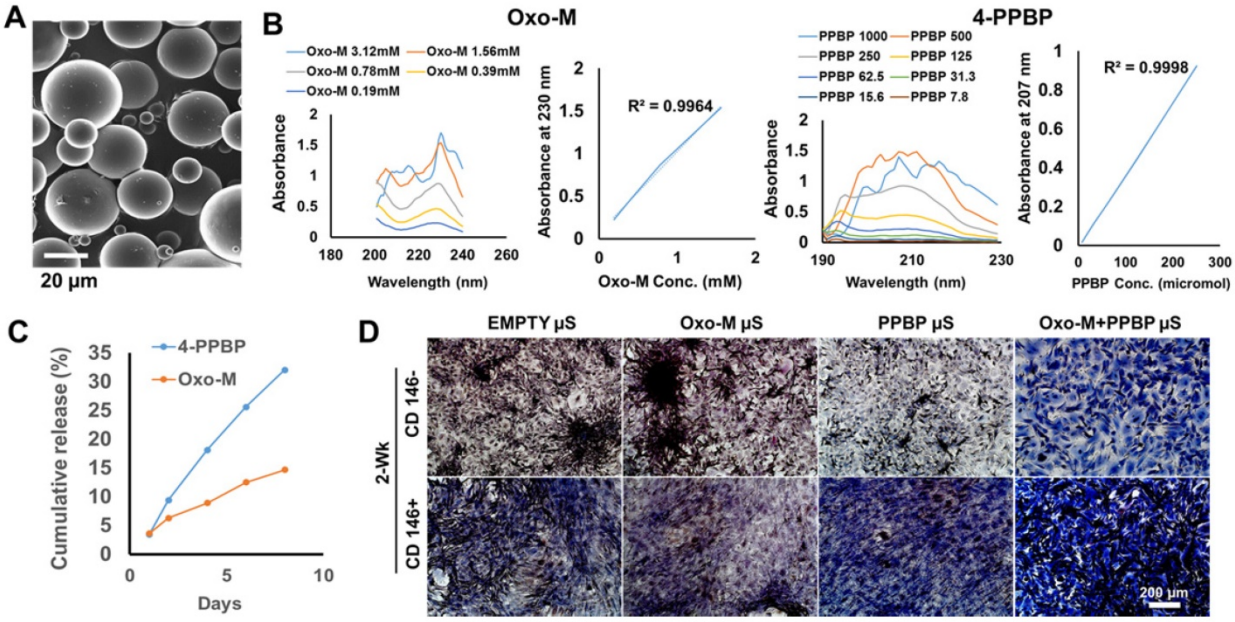

Fig. 5. Controlled delivery of of Oxo-M and 4-PPBP for tendon regeneration. Oxo-M and 4-PPBP were encapsulated in PLGA μS (**A**) by double-emulsion technique. In order to measure concentration of released Oxo-M and 4-PPBP, adsorption maxima (λ_{max}) was determined using UV-Vis spectroscopy as 230 nm and 207 nm for Oxo-M and 4-PPBP, respectively (**B**). PLGA μS provided sustained release of Oxo-M and 4-PPBP up to 7 days (**C**). A transwell co-culture experiment showed that Oxo-M and 4-PPBP released from PLGA μS increased collage deposition in CD146$^+$ TSCs by 2 wks, suggesting preservation of their bioactivities after microencapsulation (**D**).

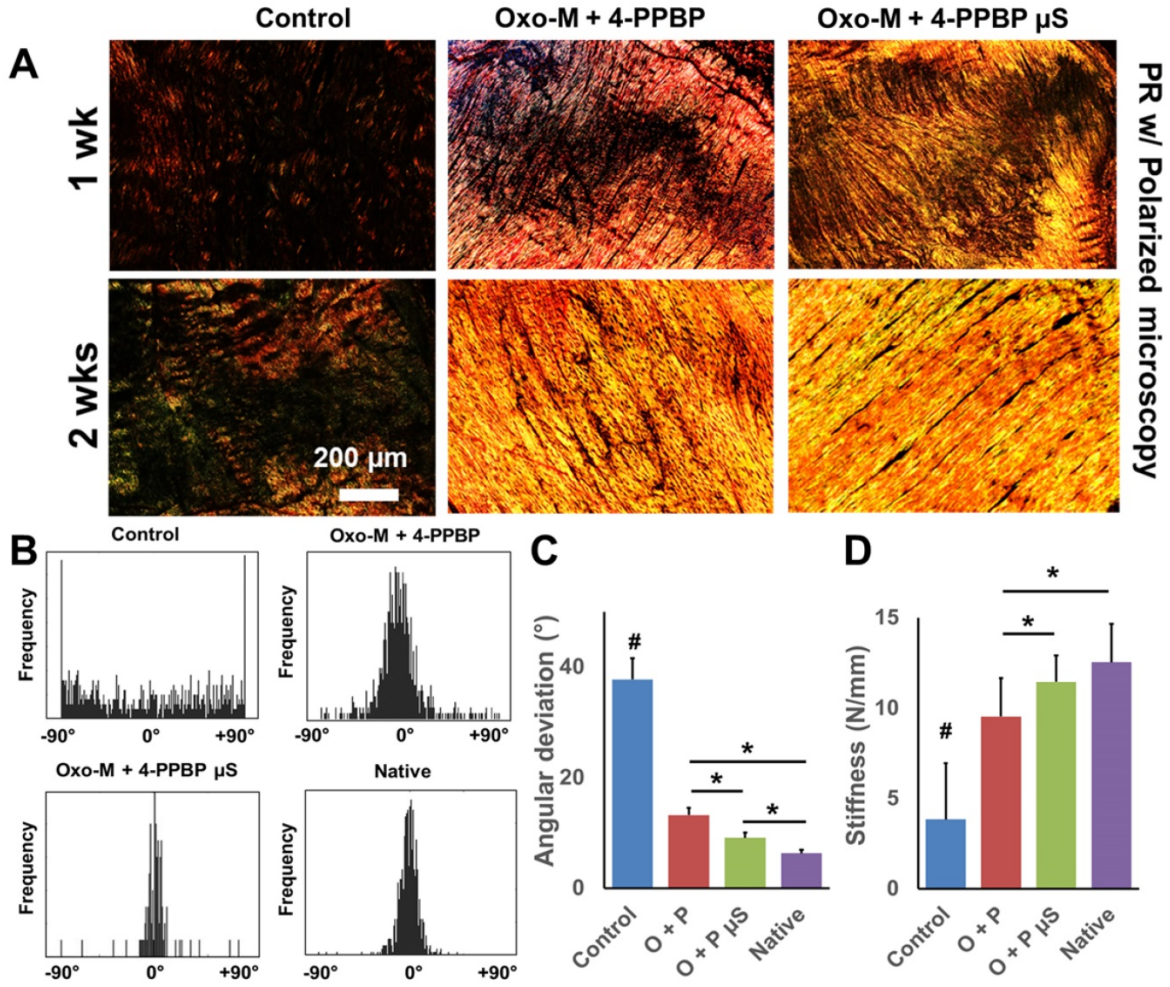

Fig. 6. Effect of controlled delivery of Oxo-M and 4-PPBP on tendon healing. By 1 and 2 wks in vivo, PR staining showed the collagen density and alignment improved with Oxo-M μS and 4-PPBP μS in comparison with direct delivery of Oxo-M and 4-PPBP via fibrin gel (**A**). Control groups ended with scar-like, disrupt collagen structure (**A**). Imaging processing of collagen fibers showed that the angular distribution of collagen fibers was narrower with Oxo-M μS and 4-PPBP μS, closer to the native level (**B**). Angular deviation (AD) was also significantly lower with Oxo-M μS and 4-PPBP μS than direct delivery of Oxo-M and 4-PPBP (**C**). Consistently, tensile stiffness of tendons delivered with Oxo-M μS and 4-PPBP μS significantly increased as compared to direct application of Oxo-M and 4-PPBP (**D**) (n = 5 per group; #: $p<0.001$ compared to all the groups, *: $p<0.01$).

Specificity of Oxo-M and 4-PPBP to CD146⁺ TSCs

Our data described above suggest that Oxo-M and 4-PPBP specifically target CD146⁺ TSCs rather than CD146⁻ other tendon cells (**Fig. 1B** and **Supplementary Fig. S2**). The specificity of the small molecules to the target stem/progenitor cells (CD146⁺ TSCs) is an important factor to consider as the potential of unexpected effects through tenocytes and/or other adjacent cells *in vivo*. Given that Oxo-M and 4-PPBP are non-selective muscarinic acetylcholine receptors (AChRs) agonist and a σ1 receptor (σ1R) ligand, respectively, we first investigated the expression patterns and roles of acetylcholine (ACh), muscarinic AChR and σ1R in CD146⁺ TSCs and CD146⁻ tendon cells. Immunofluorescence was performed with σ1R, choline acetyltransferase (ChAT; an intracellular indicator for acetylcholine synthesis), and M_1 – M_4 subtypes of AChRs in P2 - P4 rat tendon derived CD146$^{+/-}$ cells. CD146⁺ TSCs showed the stronger expressions of σ1R, ChAT, AChR M_3 and AChR M_4 as compared to CD146⁻ tendon cells (**Fig. 7A**). AChR M_1 expressed on both CD146⁺ TSCs and CD146⁻ tendon cells (**Fig. 7A**). Then we performed functional assay with application of blocking antibodies (ab) for σ1R, ChAT, AChR M_1 - M_4 with Oxo-M and 4-PPBP treatment. By 1 wk, application of σ1R-ab, AChR M_1-ab, AChR M_4-ab, and ChAT-ab significantly attenuated the tenogenic gene expressions induced by Oxo-M and 4-PPBP, including COL-I, COL-III, Tn-C, VIM, TnmD, and Scx (**Fig. 7B**) (n = 5 per group; $p<0.001$). In contrast, blocking AChR M_3 showed no significant change in the expressions of tenogenic gene markers (**Fig. 7B**). These findings suggest that ACh (indicated by ChAT), σ1R, and AChR M_1 and M_4 are closely associated with the specificity of Oxo-M and 4-PPBP to CD146⁺ TSCs.

In addition to the antibody blocking assay, we performed siRNA knockdown (KD) for σ1R, and

AChR M_1 and M_4. The other targets such as ChAT and AChR M_3 were excluded due to a low KD efficiency of the available siRNA products. The transfection efficiency was first confirmed using RFP siRNA and GAPDH siRNA with BLOCK-iT™ (ThermoFisher) (**Supplementary Fig. S3**). Transfection with BLOCK-iT™ siRNA was adopted for KD of σ1R, and AChR M_1 and M_4 rather than Silencer® siRNA used for FAK and ERK1/2 KD given a higher efficiency for the specific targets as per our pilot experiments. The KD σ1R, and AChR M_1 and M_4 significantly reduced mRNA expressions as compared to the controls (**Fig. 8A**). After 48 hours of transfection with σ1R, and AChR M_1 and M_4 siRNAs (BLOCK-iT™, ThermoFisher) (10 μM) or scrambled siRNA control (10 μM), Oxo-M and 4-PPBP were applied to $CD146^+$ TSCs and mRNA expressions of key tendon related markers, including COL-I, TnmD and SCX are measured by qRT-PCR. By 1 wk treatment of Oxo-M and 4-PPBP, σ1R and AChR M_4 KD significantly reduced the Oxo-M and 4-PPBP-elevated expressions of COL-I, COL-III, VIM and TnmD (**Fig. 8B**) (n = 5 per group; $p<0.01$). AChR M_1 KD significantly attenuated the COL-I expression but not Tn-C, VIM, TnmD and SCX (**Fig. 8B**) (n = 5 per group; $p<0.01$). The siRNA KD data showed a consistency with the antibody blocking assay except for AChR M_1, suggesting a potential time gap between the surface receptor expression and mRNA expression of AChR M_1. Moreover, AChR M_1 KD significantly increased the Tn-C and SCX expression that is likely attributed to potential intracellular cross-talks warranting additional investigations. Our signaling studies collectively suggest that Oxo-M and 4-PPBP act through AChRs and σ1R pathway, respectively, and through FAK and ERK1/2 signaling as depicted in **Figure 9**.

Discussion

The present findings strongly advocate a novel function of combined Oxo-M and 4-PPBP in tendon healing and their potential as a regenerative therapeutics. The functions of Oxo-M and 4-PPBP have been extensively investigated in the nervous system as a potential medicine to treat neuronal diseases but not for tendon or tendon stem/progenitor cells. Although Oxo-M or 4-PPBP alone showed only minimal effect, the combination of Oxo-M and 4-PPBP showed a prominent synergic effect on the induction of tenogenic differentiation of TSCs that consequently improves tendon healing *in vivo*. Since Oxo-M and 4-PPBP are ERK1/2 and FAK agonists, respectively, and ERK1/2 is a downstream of FAK signaling, the synergic effect is likely attributed to the potential cross-talk between intracellular signaling mediators associated with FAK and ERK1/2.

Despite the likely ubiquitous functions of FAK and ERK1/2 in cell proliferation, migration, differentiation and matrix synthesis, in this study, Oxo-M and 4-PPBP showed a specific targeting to $CD146^+$ TSCs rather than $CD146^-$ tendon cells in the induction of tenogenic differentiation. Since Oxo-M is a non-selective muscarinic AChR agonist [48] and

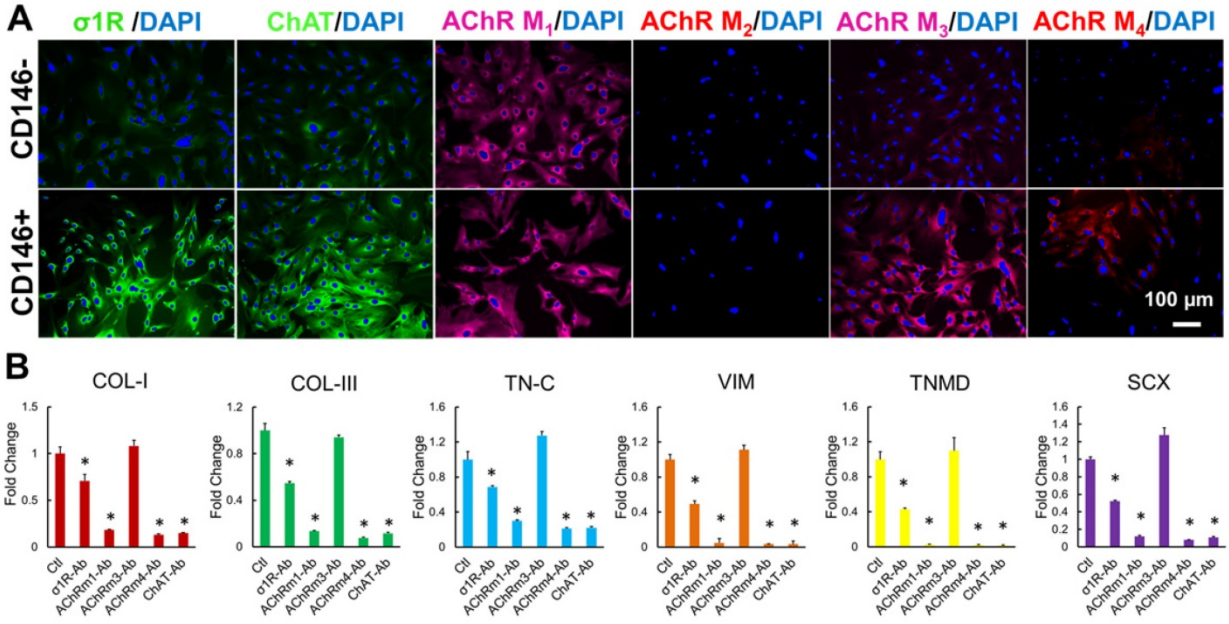

Fig. 7. Specificity of Oxo-M and 4-PPBP to CD146+ TSCs. Immunofluorescence show abundant expression of σ1R, ChAT, and AChRs M_1 - M_4 in $CD146^+$ TSC rather than $CD146^-$ tendon cells, except for AChRs M_2 (**A**). Antibody-based functional assays showed that tenogenic gene expressions by Oxo-M and 4-PPBP in TSCs were significantly attenuated by blocking σ1R, ChAT, and AChRs M_1 and M_4 (**B**) (n = 5 each group; *: $p<0.01$ compared to control).

4-PPBP is a σ1R ligand [49], we suspected ACh and σ1R signaling to be associated with the specificity of Oxo-M and 4-PPBP to the CD146$^+$ TSCs. As aligned with our hypothesis, CD146$^+$ TSCs show intrinsic expressions of σ1R, ChAT, AChR M_1 and AChR M_4 in comparison with CD146$^-$ tendon cells. Accordingly, it is suggested that the robust surface expression of σ1R in CD146$^+$ TSCs in contrast to CD146$^-$ tendon cells is responsible for the specificity of 4-PPBP on CD146$^+$ TSCs. Similarly, CD146$^+$ TSCs show the abundant expression of intracellular ChAT, an indicator of active synthesis of ACh, and the strong expressions of muscarinic ACh receptors excluding M_2 subtype. As Oxo-M is a non-selective agonist for muscarinic ACh receptors, Oxo-M may function through auto/paracrine signaling of ACh binding to M_1 and M_4 receptors, as supported by our antibody-blocking assay.

The signaling pathway of 4-PPBP bound to σ1R and ACh-to-AChRs signaling activated by Oxo-M has been extensively studied in the nervous system, primary focused on the neurotransmission [50, 51]. The roles and signaling of 4-PPBP/σ1R and Oxo-M/AChRs have rarely been investigated in non-neuronal cells with unknown secondary signaling mediators [50, 52]. Given the limited extension of the present signaling study, our follow up studies will include 1) auto/paracrine secretion of ACh and its binding to AChR M_1 and M_4, 2) determination of secondary signaling mediators that regulate tenogenic differentiation of CD146$^+$ TSCs through 4-PPBP/σ1R and Oxo-M/AChRs, and 3) their links with FAK and ERK1/2 signaling pathway. Comprehensive understanding of the intracellular signaling of Oxo-M and 4-PPBP through σ1R and AChRs potentially serve as an important foundation to achieve high efficiency and specificity of our small molecule-based regenerative therapeutics for tendon injuries and diseases.

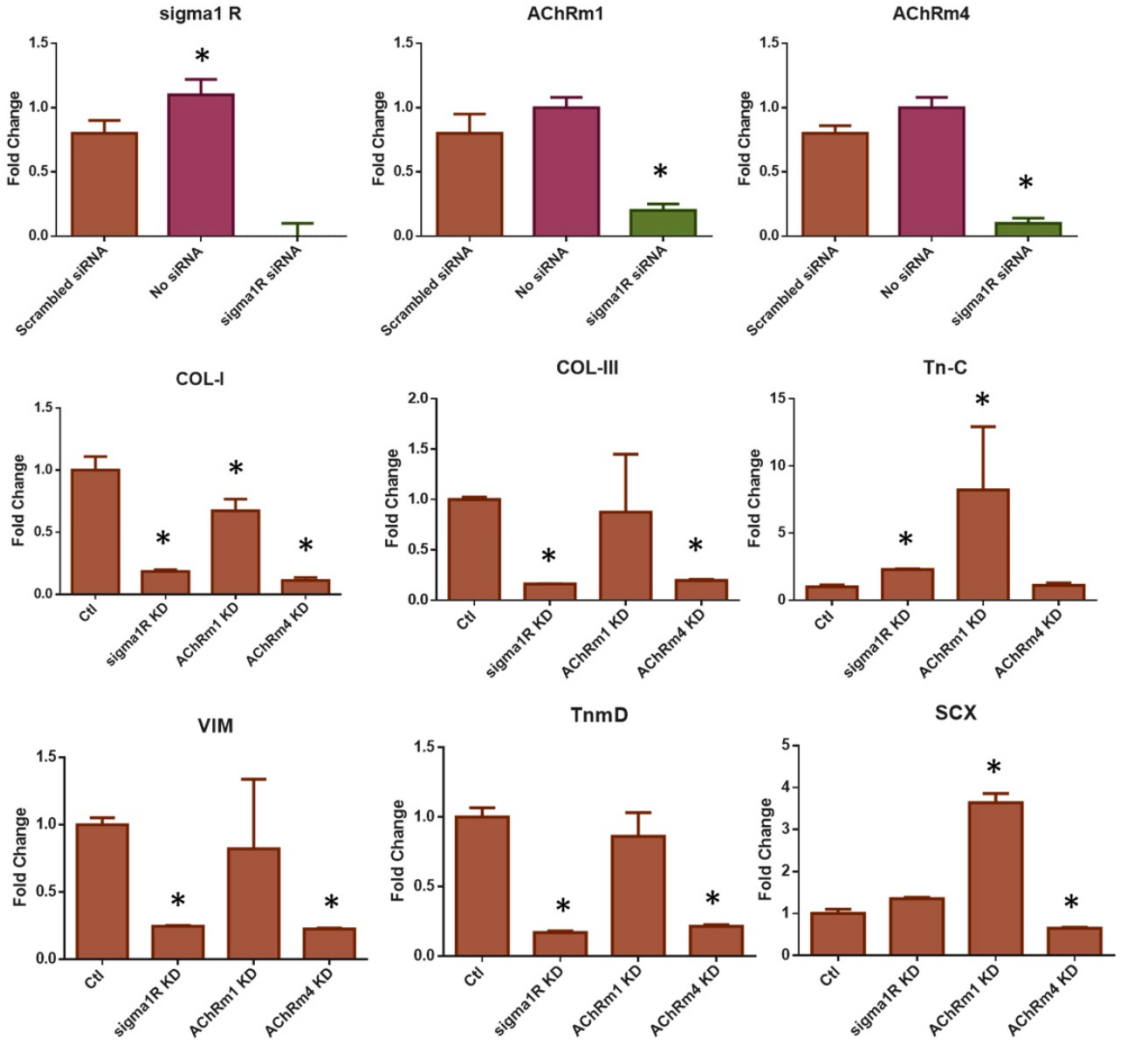

Fig. 8. The siRNA KD of σ1R and AChRs M_1 and M_4. The transfection of siRNA significantly reduced σ1R and AChRs M_1 and M_4 expressions in comparison with controls (**A**) (n = 5 per group; *p<0.001). The siRNA KD significantly reduced the Oxo-M and 4-PPBP elevated expressions of COL-I, COL-III, VIM, and TnmD by 1 wk treatment (**B**). The Tn-C and SCX and expressions were significantly lowered by AChR M_4 KD but not by σ1R KD. AChR M1 KD failed to result in significant difference in the expressions of Tn-C, VIM, TnmD and SCX (**B**) (n = 5 per group; *: p<0.01 compared to Control – scrambled siRNA).

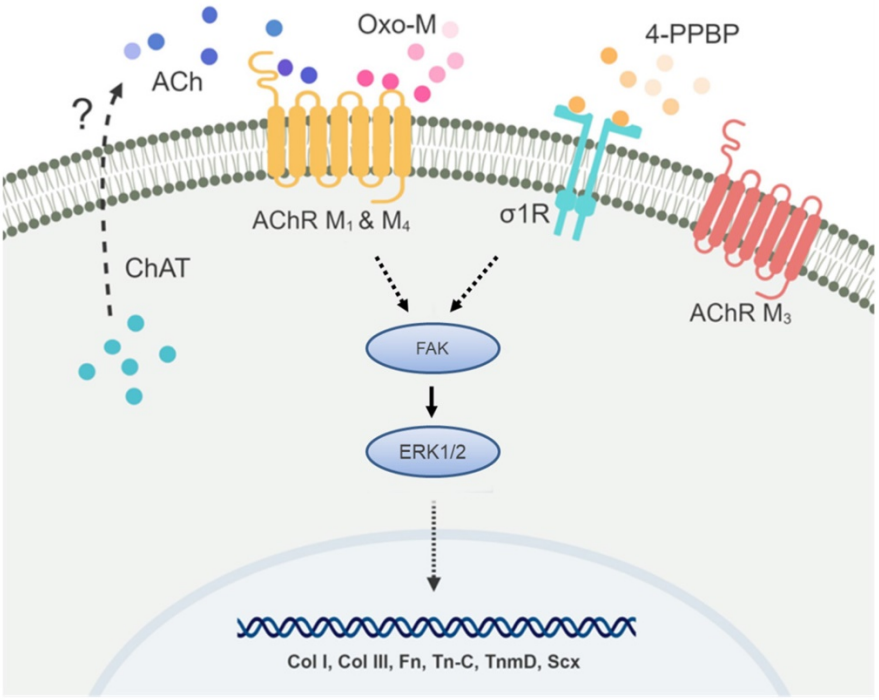

Fig. 9. Speculated mechanism for the specificity of Oxo-M and 4-PPBP to TS

Despite the promising experimental outcome both *in vitro* and *in vivo*, the present study has several limitations. First, we explored the *in vivo* effects of Oxo-M and 4-PPBP only in an acute tendon injury model. The rat PT full-transection model is valid and reproducible to study tendon healing with a clinical impact given the high incident rate. However, such acute injury model is not optimal to replicate chronic tendinopathy featured by hypercellularity, persistent inflammation, disorganized collagen fibers, increased cartilaginous matrix, decreased mechanical properties, and impaired healing. Accordingly, we will expand follow-up studies to a pathological tendon model that will address a wider range of clinical situations associated with pathological conditions in human patients. In addition, this study is limited with TSCs derived from donors with the single sex and the same age. It is well documented that sex and age are essential determinants in the incident rate of tendon injuries, tendon healing mechanism and clinical outcome [53]. In addition, a growing body of works report that sex and age influence the number, self-renewal capacity, and multipotency of TSCs [7, 54-56]. Accordingly, our future study will extend our investigation for sex and/or age difference in the efficacy of Oxo-M and 4-PPBP on TSCs' differentiation and tendon healing. Lastly, the availability of TSCs in human tendons and their regenerative capacity in response to Oxo-M and 4-PPBP are unknown, which we are currently investigating as the next translational step.

In comparison to growth factors, small molecules have a number of distinct advantages including convenience to use, no risk of cross-contamination, no immunorejection, and fine-tunable biological effects and delivery control. Oxo-M and 4-PPBP showed to be promising injectable small molecules that significantly improve tendon healing through specific targeting of endogenous tendon stem/progenitor cells. A collection of our findings demonstrated the efficiency, safety, and specificity of a combination of Oxo-M and 4-PPBP as a regenerative therapeutics for tendon injuries (**Fig. S4**). In addition, our data suggest a potential controlled delivery vehicle for Oxo-M and 4-PPBP. Taken together, the novel combination of Oxo-M and 4-PPBP, replacing the CTGF's function in tendon healing via selective signaling pathway, may have significant potential as an efficient, translational therapeutics for tendon regeneration by harnessing endogenous stem/progenitor cells (**Fig. S4**).

Materials and Methods

Study design

The overall objective and design of the study was to determine 1) the potential of the identified small molecules to stimulate tenogenic differentiation of stem/progenitor cells toward tendon regeneration and 2) the specificity and underlying mechanism of the small molecules. The primary parameters of study design included 1) the synthesis and mRNA expression of tenogenic markers with and without

small molecules and siRNA knockdown, 2) quantitative measures of collagen fibers alignment, 3) release kinetics of small molecules from PLGA μS, and 4) mechanical properties of regenerated tissues. A power analysis was performed prior to our in vitro and in vivo studies with one-way ANOVA using a level of 0.05, power of 0.8, and effect size of 1.50. The original sample size was determined as 5 biological replicates for all the in vitro experiments with cultured cells and 7 animals per group and time point, resulting in a total of 84 rats operated. By the time we performed data analysis as shown in the present manuscript, statistical significance was observed for the majority of the parameters listed above (and as reported in the manuscript). No outliers were eliminated. Endpoints were predefined as the presence or absence of statistically significant differences of the above-listed parameters. To eliminate potential person-bias for the quantitative histological analyses, we adopted an automated digital imaging processing technique, as well-established from our previous works. For the mechanical tests, we performed blind tests without providing the sample identifier to the tester.

TSC isolation and Oxo-M and 4-PPBP treatments

$CD146^+$ TSCs were isolated from patella tendons (PT) of 12 wks old Sprague-Dawley (SD) rats, as per our prior methods [13]. Briefly, the harvested PT was cleaned, minced and then digested in 2 mg/ml collagenase at 37°C for 4 hours. After centrifugation of the digest, the pellet was re-suspended in Dulbecco's Modified Eagle Medium-Low Glucose (DMEM-LG; Sigma, St. Louis, MO) containing 10% fetal bovine serum (FBS; Gibco, Invitrogen, Carlsbad, CA) and 1% penicillin-streptomycin antibiotic (Gibco, Invitrogen, Carlsbad, CA). Then $CD146^+$ cells were sorted using a magnetic cell separation kit (EasySep™, StemCells™ Technologies, Cambridge, MA). For induction of tenogenic differentiation, P1 – P2 $CD146^{+/-}$ cells at 80 – 90% confluence were treated with Oxo-M (1 mM), 4-PPBP (10 μM) or Oxo-M (1 mM) and 4-PPBP (10 μM) with medium changed every 3 days. After 2 wks treatment, quantitative RT-PCR was performed for tendon related mRNA markers including COL-I, COL-III, Tn-C, VIM, TnmD and SCX using Taqman™ assays (ThermoFisher Scientific, Waltham, MA). Controls included cells untreated and treated with 100 ng/ml CTGF. The viability of rat PT cells were tested using a live/dead cell assay upon treatment with 1X, 5X, and 10X working concentrations of Oxo-M (1 mM) and 4-PPBP (10 μM) up to 3 days as per established protocols [13, 46, 57].

Encapsulation of Oxo-M and 4-PPBP in PLGA μS for controlled delivery

For sustained release, 50 mM of Oxo-M and 500 μM of 4-PPBP were encapsulated in 250 mg of PLGA μS (75:25), respectively, following emulsification process [14, 46, 47]. In order to measure concentrations of Oxo-M and 4-PPBP with UV-Vis spectroscopy, the absorption maxima (λ_{max}) for Oxo-M (230 nm) and 4-PPBP (207 nm) were first determined, which show linear plots of absorption vs. concentration without a notable wave-length shift and noise signals. Then *in vitro* release profiles were measured by incubating 10 mg of each PLGA μS in PBS or 0.1% BSA at 37 °C with a gentle agitation. The samples were centrifuged at the selected time points, followed by measuring concentrations in the supernants with a UV-Vis spectroscope (Nanodrop™ 2000, ThermoFisher Scientific, Waltham, MA) at 230 nm and 207 nm wavelengths for Oxo-M and 4-PPBP, respectively.

Animal study and evaluation of *in vivo* outcome

Following an IACUC approved protocol, we adopted an well-established surgical model [13] for PT repair in 12 wks-old Sprague-Dawley (SD) rats (total n = 7 per group and time point; 5 for mechanical test and 2 for tissue sections). Upon creation of 10-mm longitudinal incision at medial knee and exposure of the PT, a full-thickness transverse incision was made using a no. 11 blade scalpel. Fibrin glue (50 mg/mL fibrinogen + 50 U/mL thrombin) mixed with Oxo-M (1 mM), 4-PPBP (10 μM), or Oxo-M (1 mM) + 4-PPBP (10 μM) was applied on the transection site using Fibrijet® dual injector. For the investigation of effect of sustained release of Oxo-M and 4-PPBP, Oxo-M and 4-PPBP encapsulated in PLGA μS (10 mg/ml each) were delivered to full-transected rat patella tendons (PT) mixed with fibrin gel. Control group received fibrin alone. Then a cerclage suture (2-0 Ethibond) was applied through the tibia and quadriceps to provide joint stability. The surgical site was closed using 4.0 absorbable suture (continuous stitch) for the subcutaneous layer and 4.0 PDS and monocryl suture (interrupted stitches) for the skin closure. All the animals were euthanized at 1 wk and 2 wks post-op, tendon samples were harvested for analyses as described below. The tissues harvested at 1 wk were used to evaluate the initial increase in the number of $CD146^+$ TSCs and their differentiation. The 2 wks time point was selected to evaluate collagen re-organization that represents longer-term outcome in functional tendon healing as demonstrated by our previous works [13].

Histological analysis and immunofluorescence

At 1 wk and 2 wks, tendon tissues were harvested, followed by histological analyses with H&E, Masson's Trichrome, and Picrosirius Red (PR) staining and immunofluorescence for CD146, proCOL-I, and SCX as per our prior methods [13]. Randomly selected PR stained images (n = 10 sections per tissue sample) were used to quantify collagen at the healing regions as per well-established imaging processing technique [13, 46, 57]. Total number of cells were counted using ImageJ from randomly selected slides with DAPI nucleus staining (n = 10 per group), following our existing protocols [12, 14, 46, 47]. Immunofluorescence was performed to image tissue sections using monoclonal or polyclonal antibodies and isotype-matched Alexa Fluor® secondary antibodies, with nucleus labeling with DAPI [46, 58]. All the tissue sections were made in 5-μm thickness and the antigen retrieval procedures were performed following the manufacturer's protocols. CD146 (ab75769), proCOL-I (orb222517), SCX (sc-87425), σ1R (ab53852), ChAT (ab6168), and/or AChR M_1 (ab180636), AChR M_2 (ab2805), AChR M_3 (ab87199) and AChR M_4 (ab77956) were co-labeled with multiple fluorescent secondary antibodies to show marker expressions and/or to track differentiation of endogenous TSCs. All primary antibodies and secondary antibodies were purchased from Abcam (Cambridge, MA), Santa Cruz Biotechnology (Dallas, Texas), Biorbyt (San Francisco, CA) or ThermoFisher Scientifics (Waltham, MA). All images were acquired using an inverted fluorescence microscope (Olympus IX73, Waltham, MA).

Mechanical test

Tensile tests were performed using Electroforce® Biodynamic® test system (Bose Corp., Eden Prairie, MN) following established protocols[13]. The 2 wks-harvested quadriceps-PT-tibia complexes were prepared, clamped with tensile jigs, and preconditioned for 10 cycles at 0.1 Hz between 5N and 10N while maintaining 100% humidity. Then a constant displacement rate at 0.25 mm/sec was applied until failure. Elongation was measured by the embedded displacement sensor and a Digital Video Extensometer (DVE), and force was recorded. Then the stiffness (N/mm) of each sample was calculated from the force-displacement curve. Native PT and healed PT without Oxo-M and 4-PPBP delivery served as controls.

Automated image analysis for collagen alignment

Following our prior method [13, 57], collagen fiber orientation was analyzed in PR stained tissue sections using a digital image processing technique. Briefly, the automated image-processing method was used to estimate local directionality and angular deviation (AD) in circularly polarized PR-stained images. The analysis of each image yielded a distribution of fiber orientations, ranging from -90° to 90°, where 0° was defined as the vertical direction. The degree of collagen fiber alignment was quantified using the AD. The value of the AD was calculated using circular statistics [13, 57] implemented with MATLAB (Mathworks Inc., Natick, MA, USA).

Signaling study

We first performed Western blotting to confirm phosphorylation of FAK and ERK1/2 upon Oxo-M and 4-PPBP treatment. Briefly, cellular protein was extracted from $CD146^{+/-}$ tendon cells treated with Oxo-M and/or 4-PPBP for 12 hours in RIPA Lysis Buffer (ThermoFisher Scientific, Waltham, MA) with Protease/Phosphatase Inhibitor Cocktail (Cell Signaling Technology, Danvers, MA). The proteins separated by SDS-PAGE were transferred to nitrocellulose membrane (Bio-Rad, Hercules, CA), followed by detecting with anti-phosphorylated FAK (ab81298), anti-phosphorylated ERK1/2 (sc-292838), and anti-Actin antibodies (ab8226). Images were then developed with fluorescent secondary antibodies and an infra-red fluorescence imaging system (Odyssey; LI-COR, Lincoln, NE). FAK and ERK1/2 signaling were knockdown (KD) using Silencer® siRNA (100 nM) and Neon® transfection system (ThermoFisher Scientifics, Waltham, MA) with pre-optimized electroporation conditions (1,400 V; 20 mS; 2 pulses). Scrambled siRNA was used as the negative control. FAK and ERK1/2 KD efficiency in $CD146^{+/-}$ tendon cells were confirmed using qRT-PCR by measuring mRNA expressions of FAK and ERK1/2 with commercially available Taqman™ primers (ThermoFisher).

Specificity of Oxo-M and 4-PPBP

To understand the roles of ACh, AChRs and σ1R in Oxo-M/4-PPBP-induced tenogenic differentiation of $CD146^{+}$ TSCs, we performed functional assay with antibody blocking as per our prior methods [13, 46, 59]. Briefly, P2 – P4 $CD146^{+}$ TSCs cultured on 12 well plates were incubated with blocking antibodies for σ1R (ab53852), ChAT (ab6168), AChR M_1 (ab180636), AChR M_2 (ab2805), AChR M_3 (ab87199) or AChR M_4 (ab77956) (5 μg each well), washed with PBS 3 times and then cultured with application of Oxo-M (1 mM) and 4-PPBP (10 μM). At 2 weeks, qRT-PCR was performed for the mRNA expressions of tendon-related markers, including COL-I, COL-III, Tn-C, VIM, TnmD, and SCX. The KD of σ1R, AChR

M_1 and AChR M_4 were performed by transfecting BLOCK-iT™ siRNA (ThermoFisher) using lipid based transfection (Lipofectamine™ RNAiMAX Transfection Reagent, ThermoFisher Scientific). Total 10 nM siRNA per transfection was used as per the manufacturer's protocol and a scrambled control siRNA was used as the negative control. After 48 hours of siRNA transfection and confirmation of KD efficiency, Oxo-M (1 mM) and 4-PPBP (10 μM) were applied to the transfected $CD146^+$ TSCs. At 1 wk post small molecule treatment, qRT-PCR was performed for COL-I, TnmD, and SCX using Taqman® probes (ThermoFisher Scientifics) (n = 3 biological replicates per group).

Statistical analysis

For all the quantitative data, following confirmation of normal data distribution, one-way analysis of variance (ANOVA) with post-hoc Tukey HSD tests were used with p value of 0.05. Sample sizes for all quantitative data were determined by power analysis with one-way ANOVA using a level of 0.05, power of 0.8, and effect size of 1.50 chosen to assess matrix synthesis, gene expressions, and mechanical properties in the regenerated tendon tissues and controls.

Supplementary Material

Supplementary figures.
http://www.thno.org/v09p4241s1.pdf

Acknowledgements

We thank Esther Chen, Jazmin Castillo, Michelle Skelton, and Julia Jeong for their assistance *in vitro* experiments and Jungho Back for assistance in Western blot.

Funding

This study is supported by NIH/NIAMS Grant 1R01AR071316-02 and 5R01AR065023-05 to C.H.L.

Author Contributions

S.T. was responsible for the primary technical undertaking and conducted the experiments. C.R. performed signaling study with siRNA knockdown. S.M. assisted *in vivo* animal surgeries and *in vitro* cell experiments. A.A. and R.J.Y. assisted *in vitro* signaling study and immunofluorescence. C.H.L. is responsible for the study design, data analysis and interpretation, and manuscript preparation. All the authors edited the manuscript.

Data and materials availability

All the data presented in this study will be available upon request.

Competing Interests

The authors have declared that no competing interest exists.

References

1. Arany PR, Cho A, Hunt TD, Sidhu G, Shin K, Hahm E, et al. Photoactivation of endogenous latent transforming growth factor-beta1 directs dental stem cell differentiation for regeneration. Sci Transl Med. 2014; 6: 238ra69.
2. Chen FM, Wu LA, Zhang M, Zhang R, Sun HH. Homing of endogenous stem/progenitor cells for in situ tissue regeneration: Promises, strategies, and translational perspectives. Biomaterials. 2011; 32: 3189-209.
3. Miller FD, Kaplan DR. Mobilizing endogenous stem cells for repair and regeneration: are we there yet? Cell Stem Cell. 2012; 10: 650-2.
4. Vanden Berg-Foels WS. In situ tissue regeneration: chemoattractants for endogenous stem cell recruitment. Tissue Eng Part B Rev. 2014; 20: 28-39.
5. Woo SL, Jia F, Zou L, Gabriel MT. Functional tissue engineering for ligament healing: potential of antisense gene therapy. Ann Biomed Eng. 2004; 32: 342-51.
6. Young CS, Terada S, Vacanti JP, Honda M, Bartlett JD, Yelick PC. Tissue engineering of complex tooth structures on biodegradable polymer scaffolds. J Dent Res. 2002; 81: 695-700.
7. Zhang Q, Cheng B. Tendon-derived stem cells as a new cell source for tendon tissue engineering. Front Biosci. 2013; 18: 756-64.
8. Fodor WL. Tissue engineering and cell based therapies, from the bench to the clinic: the potential to replace, repair and regenerate. Reprod Biol Endocrinol. 2003; 1: 102.
9. Mao JJ, Giannobile WV, Helms JA, Hollister SJ, Krebsbach PH, Longaker MT, et al. Craniofacial tissue engineering by stem cells. J Dent Res. 2006; 85: 966-79.
10. Prockop DJ. Repair of tissues by adult stem/progenitor cells (MSCs): controversies, myths, and changing paradigms. Mol Ther. 2009; 17: 939-46.
11. Bez M, Sheyn D, Tawackoli W, Avalos P, Shapiro G, Giaconi JC, et al. In situ bone tissue engineering via ultrasound-mediated gene delivery to endogenous progenitor cells in mini-pigs. Sci Transl Med. 2017; 9.
12. Lee CH, Cook JL, Mendelson A, Moioli EK, Yao H, Mao JJ. Regeneration of the articular surface of the rabbit synovial joint by cell homing: a proof of concept study. The Lancet. 2010; 376: 440-8.
13. Lee CH, Lee FY, Tarafder S, Kao K, Jun Y, Yang G, et al. Harnessing endogenous stem/progenitor cells for tendon regeneration. J Clin Invest. 2015; 125: 2690-701.
14. Lee CH, Rodeo SA, Fortier LA, Lu C, Erisken C, Mao JJ. Protein-releasing polymeric scaffolds induce fibrochondrocytic differentiation of endogenous cells for knee meniscus regeneration in sheep. Sci Transl Med. 2014; 6: 266ra171.
15. Lee G, Espirito Santo AI, Zwingenberger S, Cai L, Vogl T, Feldmann M, et al. Fully reduced HMGB1 accelerates the regeneration of multiple tissues by transitioning stem cells to GAlert. Proc Natl Acad Sci U S A. 2018; 115: E4463-E72.
16. Lin H, Ouyang H, Zhu J, Huang S, Liu Z, Chen S, et al. Lens regeneration using endogenous stem cells with gain of visual function. Nature. 2016; 531: 323-8.
17. Tarafder S, Gulko J, Kim D, Sim KH, Gutman S, Yang J, et al. Effect of dose and release rate of CTGF and TGFbeta3 on avascular meniscus healing. J Orthop Res. 2019.
18. Tarafder S, Gulko J, Sim KH, Yang J, Cook JL, Lee CH. Engineered Healing of Avascular Meniscus Tears by Stem Cell Recruitment. Sci Rep. 2018; 8: 8150.
19. Chen HS, Chen YL, Harn HJ, Lin JS, Lin SZ. Stem cell therapy for tendon injury. Cell Transplant. 2012.
20. Fleming BC, Spindler KP, Palmer MP, Magarian EM, Murray MM. Collagen-platelet composites improve the biomechanical properties of healing anterior cruciate ligament grafts in a porcine model. Am J Sports Med. 2009; 37: 1554-63.
21. Spindler KP, Murray MM, Devin C, Nanney LB, Davidson JM. The central ACL defect as a model for failure of intra-articular healing. J Orthop Res. 2006; 24: 401-6.
22. Tozer S, Duprez D. Tendon and ligament: development, repair and disease. Birth Defects Res C Embryo Today. 2005; 75: 226-36.
23. Voleti PB, Buckley MR, Soslowsky LJ. Tendon healing: repair and regeneration. Annu Rev Biomed Eng. 2012; 14: 47-71.
24. Chen J, Xu J, Wang A, Zheng M. Scaffolds for tendon and ligament repair: review of the efficacy of commercial products. Expert Rev Med Devices. 2009; 6: 61-73.
25. Milgrom C, Schaffler M, Gilbert S, van Holsbeeck M. Rotator-cuff changes in asymptomatic adults. The effect of age, hand dominance and gender. J Bone Joint Surg Br. 1995; 77: 296-8.
26. Tempelhof S, Rupp S, Seil R. Age-related prevalence of rotator cuff tears in asymptomatic shoulders. J Shoulder Elbow Surg. 1999; 8: 296-9.
27. Kew SJ, Gwynne JH, Enea D, Abu-Rub M, Pandit A, Zeugolis D, et al. Regeneration and repair of tendon and ligament tissue using collagen fibre biomaterials. Acta Biomater. 2011; 7: 3237-47.

28. Thomopoulos S, Williams GR, Gimbel JA, Favata M, Soslowsky LJ. Variation of biomechanical, structural, and compositional properties along the tendon to bone insertion site. J Orthop Res. 2003; 21: 413-9.
29. Juncosa-Melvin N, Boivin GP, Galloway MT, Gooch C, West JR, Butler DL. Effects of cell-to-collagen ratio in stem cell-seeded constructs for Achilles tendon repair. Tissue Eng. 2006; 12: 681-9.
30. Juncosa-Melvin N, Boivin GP, Galloway MT, Gooch C, West JR, Sklenka AM, et al. Effects of cell-to-collagen ratio in mesenchymal stem cell-seeded implants on tendon repair biomechanics and histology. Tissue Eng. 2005; 11: 448-57.
31. Juncosa-Melvin N, Matlin KS, Holdcraft RW, Nirmalanandhan VS, Butler DL. Mechanical stimulation increases collagen type I and collagen type III gene expression of stem cell-collagen sponge constructs for patellar tendon repair. Tissue Eng. 2007; 13: 1219-26.
32. Juncosa-Melvin N, Shearn JT, Boivin GP, Gooch C, Galloway MT, West JR, et al. Effects of mechanical stimulation on the biomechanics and histology of stem cell-collagen sponge constructs for rabbit patellar tendon repair. Tissue Eng. 2006; 12: 2291-300.
33. Nirmalanandhan VS, Shearn JT, Juncosa-Melvin N, Rao M, Gooch C, Jain A, et al. Improving linear stiffness of the cell-seeded collagen sponge constructs by varying the components of the mechanical stimulus. Tissue Eng Part A. 2008; 14: 1883-91.
34. Nourissat G, Diop A, Maurel N, Salvat C, Dumont S, Pigenet A, et al. Mesenchymal stem cell therapy regenerates the native bone-tendon junction after surgical repair in a degenerative rat model. PLoS One. 2010; 5: e12248.
35. Ouyang HW, Cao T, Zou XH, Heng BC, Wang LL, Song XH, et al. Mesenchymal stem cell sheets revitalize nonviable dense grafts: implications for repair of large-bone and tendon defects. Transplantation. 2006; 82: 170-4.
36. Fan H, Liu H, Toh SL, Goh JC. Anterior cruciate ligament regeneration using mesenchymal stem cells and silk scaffold in large animal model. Biomaterials. 2009; 30: 4967-77.
37. Fan H, Liu H, Wong EJ, Toh SL, Goh JC. In vivo study of anterior cruciate ligament regeneration using mesenchymal stem cells and silk scaffold. Biomaterials. 2008; 29: 3324-37.
38. Hsu SL, Liang R, Woo SL. Functional tissue engineering of ligament healing. Sports Med Arthrosc Rehabil Ther Technol. 2010; 2: 12.
39. Devana SK, Kelley BV, McBride OJ, Kabir N, Jensen AR, Park SJ, et al. Adipose-derived Human Perivascular Stem Cells May Improve Achilles Tendon Healing in Rats. Clin Orthop Relat Res. 2018; 476: 2091-100.
40. Goncalves AI, Gershovich PM, Rodrigues MT, Reis RL, Gomes ME. Human adipose tissue-derived tenomodulin positive subpopulation of stem cells: A promising source of tendon progenitor cells. J Tissue Eng Regen Med. 2018; 12: 762-74.
41. Shen H, Jayaram R, Yoneda S, Linderman SW, Sakiyama-Elbert SE, Xia Y, et al. The effect of adipose-derived stem cell sheets and CTGF on early flexor tendon healing in a canine model. Sci Rep. 2018; 8: 11078.
42. Butler DL, Gooch C, Kinneberg KR, Boivin GP, Galloway MT, Nirmalanandhan VS, et al. The use of mesenchymal stem cells in collagen-based scaffolds for tissue-engineered repair of tendons. Nat Protoc. 2010; 5: 849-63.
43. Li W, Li K, Wei W, Ding S. Chemical approaches to stem cell biology and therapeutics. Cell Stem Cell. 2013; 13: 270-83.
44. Linseman DA, Sorensen SD, Fisher SK. Attenuation of focal adhesion kinase signaling following depletion of agonist-sensitive pools of phosphatidylinositol 4,5-bisphosphate. J Neurochem. 1999; 73: 1933-44.
45. Gutman S, Kim D, Tarafder S, Velez S, Jeong J, Lee CH. Regionally variant collagen alignment correlates with viscoelastic properties of the disc of the human temporomandibular joint. Arch Oral Biol. 2018; 86: 1-6.
46. Lee CH, Shah B, Moioli EK, Mao JJ. CTGF directs fibroblast differentiation from human mesenchymal stem/stromal cells and defines connective tissue healing in a rodent injury model. J Clin Invest. 2010; 120: 3340-9.
47. Lee CH, Marion NW, Hollister S, Mao JJ. Tissue formation and vascularization in anatomically shaped human joint condyle ectopically in vivo. Tissue Eng Part A. 2009; 15: 3923-30.
48. Rinaldo L, Hansel C. Muscarinic acetylcholine receptor activation blocks long-term potentiation at cerebellar parallel fiber-Purkinje cell synapses via cannabinoid signaling. Proc Natl Acad Sci U S A. 2013; 110: 11181-6.
49. Wegleiter K, Hermann M, Posod A, Wechselberger K, Stanika RI, Obermair GJ, et al. The sigma-1 receptor agonist 4-phenyl-1-(4-phenylbutyl) piperidine (PPBP) protects against newborn excitotoxic brain injury by stabilizing the mitochondrial membrane potential in vitro and inhibiting microglial activation in vivo. Exp Neurol. 2014; 261: 501-9.
50. Bjur D, Danielson P, Alfredson H, Forsgren S. Presence of a non-neuronal cholinergic system and occurrence of up- and down-regulation in expression of M2 muscarinic acetylcholine receptors: new aspects of importance regarding Achilles tendon tendinosis (tendinopathy). Cell Tissue Res. 2008; 331: 385-400.
51. Rousseaux CG, Greene SF. Sigma receptors [sigmaRs]: biology in normal and diseased states. J Recept Signal Transduct Res. 2015: 1-62.
52. Fong G, Backman LJ, Andersson G, Scott A, Danielson P. Human tenocytes are stimulated to proliferate by acetylcholine through an EGFR signalling pathway. Cell Tissue Res. 2013; 351: 465-75.
53. Magnusson SP, Hansen M, Langberg H, Miller B, Haraldsson B, Westh EK, et al. The adaptability of tendon to loading differs in men and women. Int J Exp Pathol. 2007; 88: 237-40.
54. Zhang J, Wang JH. Moderate Exercise Mitigates the Detrimental Effects of Aging on Tendon Stem Cells. PLoS One. 2015; 10: e0130454.
55. Zhang X, Lin YC, Rui YF, Xu HL, Chen H, Wang C, et al. Therapeutic Roles of Tendon Stem/Progenitor Cells in Tendinopathy. Stem Cells Int. 2016; 2016: 4076578.
56. Zhou Z, Akinbiyi T, Xu L, Ramcharan M, Leong DJ, Ros SJ, et al. Tendon-derived stem/progenitor cell aging: defective self-renewal and altered fate. Aging Cell. 2010; 9: 911-5.
57. Lee CH, Shin HJ, Cho IH, Kang YM, Kim IA, Park KD, et al. Nanofiber alignment and direction of mechanical strain affect the ECM production of human ACL fibroblast. Biomaterials. 2005; 26: 1261-70.
58. Yang R, Chen M, Lee CH, Yoon R, Lal S, Mao JJ. Clones of Ectopic Stem Cells in the Regeneration of Muscle Defects in Vivo. PLoS ONE. 2010; In press.
59. Lee CH, Hajibandeh J, Suzuki T, Fan A, Shang P, Mao JJ. Three-dimensional printed multiphase scaffolds for regeneration of periodontium complex. Tissue Eng Part A. 2014; 20: 1342-51.